Journal of Power Sources 189 (2009) 823–827

Contents lists available at ScienceDirect

Journal of Power Sources

journal homepage: www.elsevier.com/locate/jpowsour

Short communication

On the use of transition metal oxysalts as conversion electrodes in lithium-ion batteries

María José Aragón, Bernardo León, Carlos Pérez Vicente, José L. Tirado*

Laboratorio de Química Inorgánica, Universidad de Córdoba, Edificio C3, Campus de Rabanales, 14071 Córdoba, Spain

ARTICLE INFO

Article history:
Received 19 June 2008
Received in revised form 21 July 2008
Accepted 21 July 2008
Available online 26 July 2008

Keywords:
Conversion electrodes
Lithium batteries
Iron oxalate
Manganese carbonate

ABSTRACT

Transition metal oxysalts are evaluated as conversion electrode material. Anhydrous iron oxalate is investigated and a comparison with manganese carbonate is carried out to envisage the possible extension of these studies to a vast number of transition metal oxysalts. The dehydration process is studied by thermal analysis to prepare the anhydrous oxysalts. Both manganese carbonate and iron oxalate are interesting candidates for the active material of the negative electrode of lithium-ion batteries. A higher reversible capacity and lower irreversible capacity are observed for the oxalate compound. The reversible capacity cannot be exclusively ascribed to redox processes involving iron. The low temperature synthesis of these materials makes them an inexpensive option for this purpose.

1. Introduction

In the last decade, a renewed enthusiasm on the potential use of transition metal oxides as active electrode material for lithium-ion batteries was developed [1]. First-row transition metal oxides such as cobalt, iron and copper oxides with different M:O ratios were soon examined [2–6]. Prominent reversible electrode capacities up to ca. 800 mAh g^{-1}, at voltages around 1 V vs. lithium were detected, together with a good response on prolonged cycling and acceptable rate performance. In addition, their environmental friendship and low cost are also attractive properties for a future use spreading.

In binary transition metal oxides, the electrochemical conversion reaction goes through a first main process in which metal reduction and oxide anion transfer from the transition metal to lithium ions take place. A second step involves the formation of an organic polymeric layer, a process in which electrochemical reversibility has been demonstrated [5]. The strongly exoergic nature of the conversion reaction, which can be deduced from standard Gibbs free energy values, was initially taken as an argument to discard the practical feasibility of the reversible reaction, and Li_2O was considered electrochemical inactive. The profound structural degradation that takes place during the conversion reaction leads to nanodispersed particles of the solid products at the end of the reduction process. The resulting enhanced surface energy can be considered as a main factor favoring the electrochemical reversibility. Moreover, the catalytic effect of the transition metal also affords for the Li_2O reversibility [7]. This effect was also evidenced for transition metal mixed oxides, in which a variable extension of the reduction–reoxidation processes was found for each transition element [8–11].

In addition, conversion reactions have also been detected for other anions as sulphides [12], nitrides [13], and transition metal fluorides have been proposed for the positive electrode [14,15]. Also, the development of suitable synthesis procedure to produce particle size and morphologies to improve the electrode performance have been studied in detail. Additional improvements are however needed. Thus, hysteresis phenomena on charge–discharge cycles, capacity fading, and optimum rate performance are still subjects of improvement.

Recently, we were able to find a similar reversible electrochemical response in submicrometric particles of manganese carbonate with the calcite structure [16]. This study revealed that $MnCO_3$ can be used directly as a conversion electrode vs. lithium. The discharge of lithium test cells takes place by a different conversion reaction than that observed for the oxide produced during the thermal decomposition of the carbonate, MnO. Similar values of reversible capacity and better capacity retention were observed for the carbonate, as compared with the oxide.

In this work, the study of oxysalts as conversion electrode material is investigated for one additional compound, iron oxalate. A comparison with manganese carbonate is carried out to envisage

* Corresponding author. Tel.: +34 957218637.
E-mail address: iq1ticoj@uco.es (J.L. Tirado).

0378-7753/$ – see front matter © 2008 Elsevier B.V. All rights reserved.
doi:10.1016/j.jpowsour.2008.07.046

the possible extension of these studies to a vast number of transition metal oxysalts.

2. Experimental

The synthesis of $MnCO_3$ submicronic particles was carried out from microemulsions of water in cyclohexane, stabilized with AOT, (sodium bis(ethylhexyl) sulfosuccinate) surfactant [16]. Commercial iron oxalate was provided by Panreac (Barcelona). Both solids were dehydrated under the experimental conditions discussed below.

X-ray diffraction (XRD) patterns were recorded on a Siemens D5000, using Cu Kα radiation and a graphite monochromator. Transmission electron microscopy (TEM) images were obtained with a JEOL 200CX microscope. Thermogravimetric (TG) and differential thermal analysis (DTA) curves were obtained in a SHIMADZU DTG-60AH instrument in both air and argon atmosphere.

For electrochemical tests, two-electrode Swagelok-type cells were used. The electrodes were prepared by blending the powdered active material (60%) with carbon black (30%), and poly-vinylidene fluoride (10%) dissolved in *N*-methyl-pyrrolidone. The slurry was cast onto a Cu foil and vacuum dried at 200 °C. As the negative electrode, a lithium foil was used. The electrolyte was a solution of ethylene carbonate–diethyl carbonate in 1:1 weight proportion, including 1 M $LiPF_6$, supported by a porous glass-paper Whatman disk. The cells were assembled in an Ar-filled glove box (H_2O, O_2 < 1 ppm). Galvanostatic charge/discharge cycles were carried out with the aid of a multichannel MacPile II system, at different *C* rates ($C = 1\ Li\ h^{-1}\ mol^{-1}$).

3. Results and discussion

The as-received commercial iron oxalate was crystallized with two water molecules. Thermogravimetric curves (Fig. 1, upper) were recorded to locate the best temperature and experimental conditions at which the two water molecules are released from $FeC_2O_4{\cdot}2H_2O$ without breakage of the oxalate anion. The observed weight loss in the dehydration step at 210 °C agrees perfectly with the theoretical value of Eq. (1) (20.02%). The processes following dehydration are written in Eqs. (2) and (3), which globally account for the main exotherm in the DTA curve and the weight loss (44.5% referred to anhydrous FeC_2O_4) at 270 °C.

$$FeC_2O_4{\cdot}2H_2O \rightarrow FeC_2O_4 + 2H_2O \quad (1)$$

$$FeC_2O_4 \rightarrow FeO + CO + CO_2 \quad (2)$$

$$2FeO + 1/2O_2 \rightarrow Fe_2O_3 \quad (3)$$

Obviously, reaction (3) did not take place under an inert atmosphere and the of the weight loss temperature of reactions (1) and (2) decreased by ca. 10 °C.

In turn, the thermal decomposition of manganese carbonate takes place by different steps in the thermogravimetric curve (Fig. 1, lower), according to:

$$MnCO_3 + 3/2O_2 \rightarrow MnO_2 + 2CO_2 \quad (4)$$

$$2MnO_2 \rightarrow Mn_2O_3 + 1/2O_2 \quad (5)$$

$$3Mn_2O_3 \rightarrow 2Mn_3O_4 + 1/2O_2 \quad (6)$$

Under an inert atmosphere, the decomposition process takes place in a single step, leading to MnO and CO_2 [16].

The theoretical weight changes corresponding to each reaction agree well with the steps in the experimental TG curve. In addition, the occurrence of an initial weight loss until about 150 °C is associated with the loss of water molecules weakly bound to the outer surface of the manganese carbonate particles. The existence of surface water is linked to the fact that the precipitation of carbonate took place in an aqueous medium within the volume of water droplets in the stabilized emulsions used by the reverse micelles method. Moreover, the high specific surface resulting from the ultrafine dispersion of the subnanometric solid favors the existence of substantial amounts of adsorbed water.

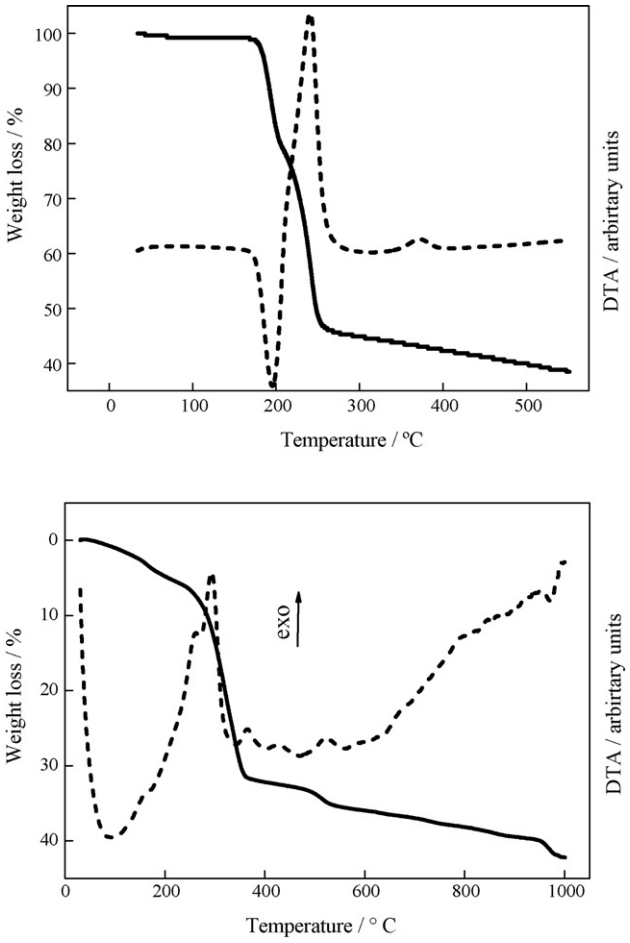

Fig. 1. TG–DTA curves in air of $FeC_2O_4{\cdot}2H_2O$ (upper) and $MnCO_3$ (lower).

Thus, previously to the electrochemical experiments, $FeC_2O_4{\cdot}2H_2O$ and $MnCO_3$ were dehydrated at 200 °C for 8 h and 300 °C for 3 h, respectively, in the absence of O_2. In order to confirm that the dehydration of iron oxalate took place without breakage of the oxyanion, the XRD patterns of the dehydrated iron product were recorded and were congruent with a poorly crystalline solid with FeC_2O_4 composition [17], while $MnCO_3$ remained basically unaffected. Moreover, the TG–DTA experiments of the dehydrated materials exactly reproduced the second part of the curves in Fig. 1.

Fig. 2 shows the electron micrographs of both dehydrated products. Iron oxalate appears as large particles of several micrometers with a complex mesoporous texture, due to the release of crystallization water molecules during dehydration at 200 °C. In contrast, the carbonate particles have the same regular submicrometric shape previously described [5] without extra porosity, thus showing that the weight loss up to 300 °C corresponds to weakly bond surface water.

The electrochemical reaction with lithium of both anhydrous $MnCO_3$ and FeC_2O_4 took place with a first extended plateau (ca. 1500 mAh g^{-1} see Fig. 3). However, the voltage profile differs

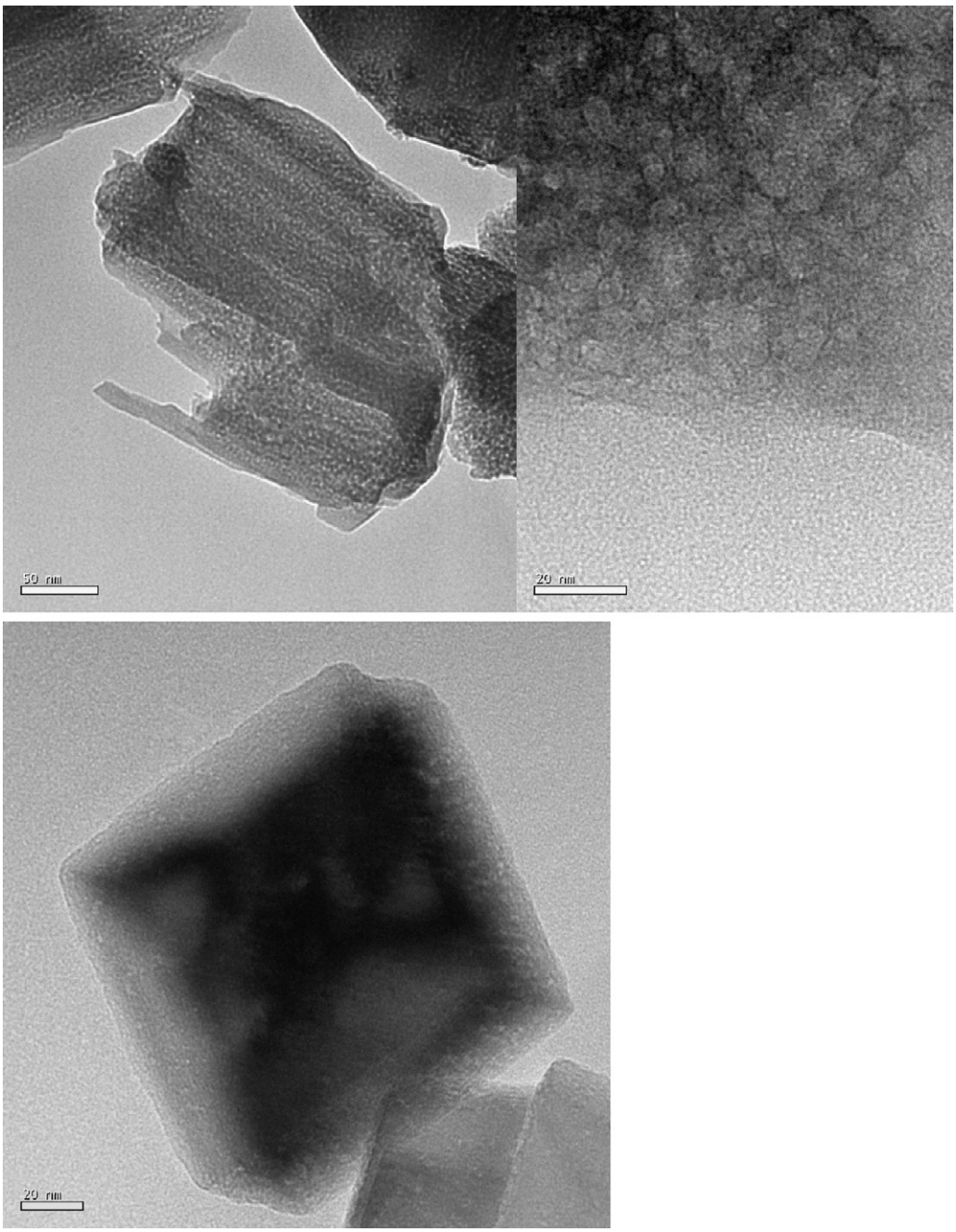

Fig. 2. TEM images of dehydrated products at 200 °C, FeC_2O_4 (upper), and 300 °C, $MnCO_3$ (lower).

notably. For FeC_2O_4 a first extended plateau at ca. 1.2 V vs. Li is observed, followed by a smooth decrease in voltage until 0 V. In contrast, the voltage profile for the carbonate shows a small plateau at ca. 0.9 V and a second extended plateau at ca. 0.4 V. Irrespective of these differences, both oxysalts lead to X-ray amorphous products after the first discharge and crystallinity was not recovered during further cycles. Nevertheless, by analogy with previous conversion electrode materials the first step can be associated to the formation of iron and manganese metal. An in-depth ^{57}Fe Mössbauer spectroscopy and XAS study is being developed to account for this interpretation. Preliminary results suggest that iron metal nanoparticles are present in the electrode after the first discharge. Then, for each oxysalt electrode material, the first discharge in lithium test cells can be mainly ascribed to the following reactions:

$$FeC_2O_4 + 2Li^+ + 2e^- \rightarrow Fe + Li_2C_2O_4 \quad (7)$$

$$MnCO_3 + 2Li^+ + 2e^- \rightarrow Mn + Li_2CO_3 \quad (8)$$

The theoretical capacity values calculated for reactions (7) and (8) are 372 and 466 mAh g^{-1}, respectively. Thus there is a huge extra irreversible capacity that could be ascribed to both the formation of a SEI and extended electrolyte degradation. The initial irreversible capacity of the oxalate (ca. 300 mAh g^{-1}) is lower than that corresponding to $MnCO_3$, (ca. 800 mAh g^{-1}) although it is still large and has to be avoided for a practical application of these electrode materials. The differences between iron and manganese compounds are

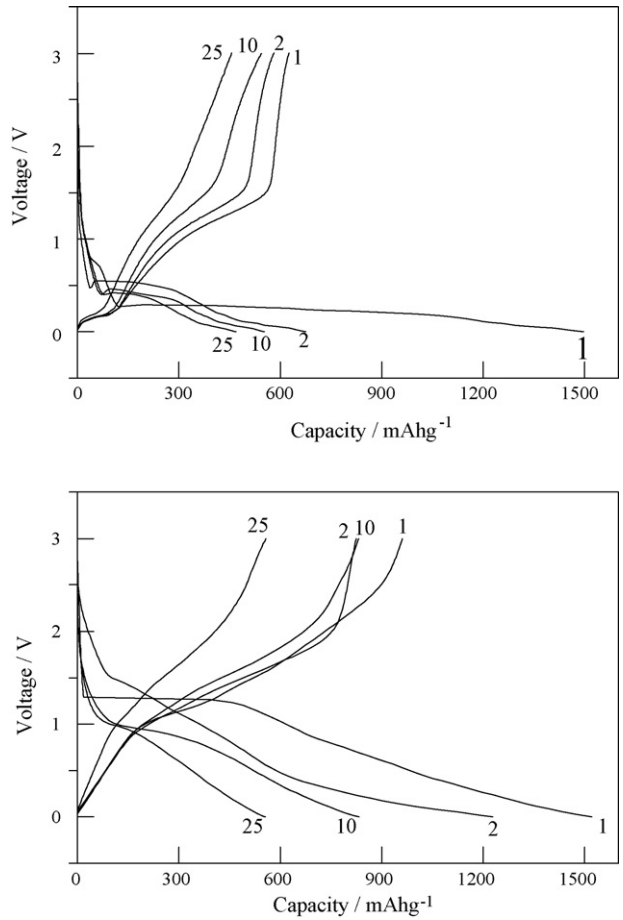

Fig. 3. Charge–discharge branches of lithium test cells using as initial active cathode material FeC_2O_4 (upper) and $MnCO_3$ (lower).

connected with the enhanced extension of the low-voltage plateau during the first discharge of $MnCO_3$. This could be a consequence of a different catalytic effect of manganese as compared with iron metal nanoparticles [7].

The following cycles were found to be reversible. Fig. 4 shows the rate performance of iron oxalate. The initial capacity is significantly lower at high rate, while extended cycling reveals excellent capacity

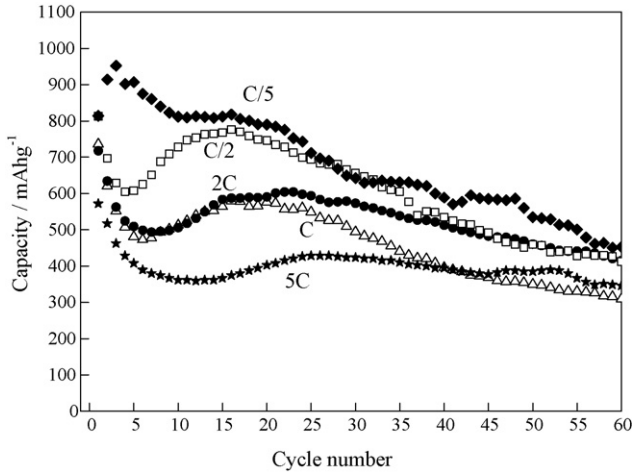

Fig. 4. Capacity vs. cycle number of lithium cells using FeC_2O_4 electrode material at different *C* rates.

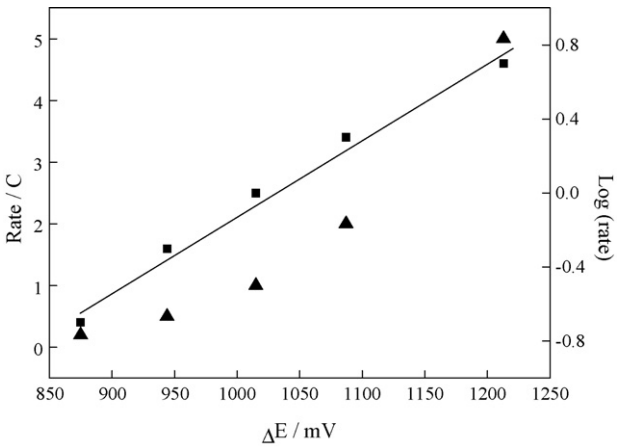

Fig. 5. Plot of *C*-rate vs. hysteresis (ΔE) for lithium cells using FeC_2O_4 electrode material.

retention for 5C. In consequence, the values observed at 50 cycles or higher are rather close for the different rates.

On the other hand, significant hysteresis phenomena are observed in Fig. 3, which is also common feature in conversion electrodes. The experimental results obtained in this study reveal that the hysteresis observed in manganese carbonate electrodes is commonly less marked than in related oxides, which is a positive result with a view of a potential application of these materials. However, the difference is favorable to iron oxalate. In order to gain further insight on the origin of the hysteresis phenomena, the different rate values are plotted against the differences in cell potential of the charge and discharge branches (ΔE). It can be observed the magnitude of the hysteresis phenomenon increases with rate, and also with current density as sample weights in the electrode were equivalent. Moreover, in the logarithmic scale, an Arrhenius behaviour it is clearly observed (straight line in Fig. 5). These results agree well with an excellent study on the electrochemical system Fe_3O_4, which was found to behave as impedance with an activation step and not as a pure resistance [6]. The reaction is then governed by mass transfer through grain boundaries between the three solid-state components during the charge/discharge processes. The differences between carbonate/oxalate and oxide suggest that one of the components is the lithium oxysalt instead of Li_2O, with different ion mobility. Similar differences in ΔE have been described when phosphides and fluorides are used instead of oxides [6].

The cycle performance at C/4 of both oxysalts is compared in Fig. 6. Iron oxalate shows higher capacities than manganese carbonate. This is also observed even when iron oxalate is cycled at higher rate. Thus, capacities were always above 700 mAh g^{-1} up to 25 cycles when iron oxalate was cycled at C/2 rate (Fig. 4). The reversible capacity values for the oxalate contrast markedly with the theoretical capacity of reaction (7). Different origins of this discrepancy could be:

- The oxidation reaction is not coincident with the reverse Eq. (7), iron being oxidized to Fe(III) oxides on cell charge.
- The possible reversible formation of an “organic” layer such as that described by Tarascon and co-workers [5] enhanced by the composition of the composite material (metal plus lithium oxysalts).
- A contribution of capacitative effects, which is particularly favored by the mesoporous texture of the oxalate particles.

At present none of these effects can be fully discarded. Further studies are now in progress.

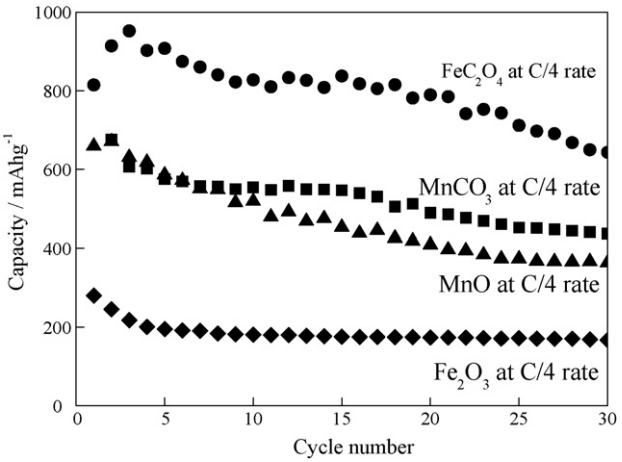

Fig. 6. Capacity vs. cycle number of lithium cells using $MnCO_3$ and FeC_2O_4 electrode materials and decomposition oxide products.

Moreover, if the capacity values are compared with the behaviour of oxides derived from the oxysalts for the same C/4 rate (also included in Fig. 6), a higher capacity is still observed for the undecomposed solids.

4. Conclusions

The main conclusion of this study is that first-row transition metal oxysalts are potential candidates for the active material of the negative electrode of lithium-ion batteries. The low temperature dehydration synthesis of these solids makes them an inexpensive option to obtain high-capacity active materials. In addition the use of less toxic and contaminant materials by avoiding cobalt gives additional advantages to this option. A comparison between manganese carbonate submicrometric particles and iron oxalate of commercial origin shows that the iron compound surpasses the carbonate performance in lithium test cells, with reversible capacities above 700 mAh g^{-1}, and good capacity retention at high rates.

Acknowledgements

The authors acknowledge financial support from Junta de Andalucía (contract FQM1447), MEC (contract MAT2005-00374). MJA is indebted to MEC for an FPI grant.

References

[1] P. Poizot, P.S. Laruelle, S. Grugeon, S.L. Dupont, J.-M. Tarascon, Nature 407 (2000) 496.
[2] S. Grugeon, S. Laruelle, R. Herrera-Urbina, L. Dupont, P. Poizot, J.-B. Leriche, J.M. Tarascon, J. Electrochem. Soc. 148 (2001) A285.
[3] P. Poizot, S. Laruelle, S. Grugeon, J.M. Tarascon, J. Electrochem. Soc. 149 (2002) A1212.
[4] D. Larcher, D. Bonnin, R. Cortes, I. Rivals, L. Personnaz, J.-M. Tarascon, J. Electrochem. Soc. 150 (2003) A1643.
[5] A. Débart, L. Dupont, P. Poizot, J.-B. Leriche, J.M. Tarascon, J. Electrochem. Soc. 148 (2001) A1266.
[6] P.L. Taberna, S. Mitra, P. Poizot, P. Simon, J.-M. Tarascon, Nature Mater. 5 (2006) 567.
[7] Y.-M. Kang, M.-S. Song, J.-H. Kim, H.-S. Kim, M.-S. Park, J.-Y. Lee, H.K. Liu, S.X. Dou, Electrochim. Acta 50 (2005) 3667.
[8] R. Alcántara, M. Jaraba, P. Lavela, J.L. Tirado, Chem. Mater. 14 (2002) 2847.
[9] R. Alcántara, M. Jaraba, P. Lavela, J.L. Tirado, J.C. Jumas, J. Olivier-Fourcade, Electrochem. Commun. 5 (2003) 16.
[10] A. Chadwick, S.L.P. Savin, S. Fiddy, R. Alcántara, D. Fernández Lisbona, Pedro Lavela, G.F. Ortiz, J.L. Tirado, J. Phys. Chem. C 111 (2007) 4636.
[11] P. Lavela, J.L. Tirado, J. Power Sources 172 (2007) 379.
[12] Y. Shao-Horn, S. Osmialowski, Q.C. Horn, J. Electrochem. Soc. 149 (2002) A1547.
[13] T. Shodai, S. Okada, S. Tobishma, J. Yamaki, J. Power Sources 68 (1997) 515.
[14] F. Badway, A.N. Mansour, N. Pereira, J.F. Al-Sharab, F. Cosandey, I. Plitz, G.G. Amatucci, Chem. Mater. 19 (2007) 4129.
[15] P. Liao, B.L. MacDonald, R.A. Dunlap, J.R. Dahn, Chem. Mater. 20 (2008) 454.
[16] M.J. Aragón, C. Pérez-Vicente, J.L. Tirado, Electrochem. Commun. 9 (2007) 1744.
[17] R.A. Brown, S.C. Bevant, J. Inorg. Nucl. Chem. 28 (1966) 387.